PROCEEDINGS OF SPIE

SPIEDigitalLibrary.org/conference-proceedings-of-spie

Engineering Kerr-cat qubits for hardware efficient quantum error correction

Xu, Qian, Putterman, Harald, Iverson, Joseph, Noh, Kyungjoo, Painter, Oskar, et al.

Qian Xu, Harald Putterman, Joseph K. Iverson, Kyungjoo Noh, Oskar J. Painter, Fernando G. S. L. Brandao, Liang Jiang, "Engineering Kerr-cat qubits for hardware efficient quantum error correction," Proc. SPIE 12015, Quantum Computing, Communication, and Simulation II, 120150B (1 March 2022); doi: 10.1117/12.2614832

SPIE.

Event: SPIE OPTO, 2022, San Francisco, California, United States

Invited Paper

Engineering Kerr-cat qubits for hardware efficient quantum error correction

Qian Xu[1, 2], Harald Putterman[2, 3], Joseph K Iverson[2, 3], Kyungjoo Noh[2, 3], Oskar Painter[2, 3], Fernando G.S.L. Brandão[2, 3], and Liang Jiang[1, 2]

[1]Pritzker School of Molecular Engineering, The University of Chicago, Illinois 60637, USA
[2]AWS Center for Quantum Computing, Pasadena, CA 91125, USA
[3]IQIM, California Institute of Technology, Pasadena, CA 91125, USA

ABSTRACT

Stabilized cat qubits that possess biased noise channel with bit-flip errors exponentially smaller than phase-flip errors. Together with a set of bias-preserving (BP) gates, cat qubits are a promising candidate for realizing hardware efficient quantum error correction and fault-tolerant quantum computing. Compared to dissipatively stabilized cat qubits, the Kerr cat qubits can in principle support faster gate operations with higher gate fidelity, benefiting from the large energy gap that protects the code space. However, the leakage of the Kerr cats can increase the minor type of errors and compromise the noise bias. Both the fast implementation of gates and the interaction with environment can lead to such detrimental leakage if no sophisticated controls are applied. In this work, we introduce new fine-control techniques to overcome the above obstacles for Kerr cat qubits. To suppress the gate leakage, we use the derivative-based transition suppression technique to design derivative-based controls for the Kerr BP gates. We show that the fine-controlled gates can simultaneously have high gate fidelity and high noise bias and when applied to concatenated quantum error correction, can not only improve the logical error rate but also reduce resource overhead. To suppress the environment-induced leakage, we introduce colored single-photon dissipation, which can continuously cool the Kerr cats and suppress the minor errors while not enhancing the major errors.

1. INTRODUCTION

Quantum error correction (QEC) of generic errors is very challenging, because of the demanding threshold requirements and significant resource overhead. To overcome this challenge, we may adaptively design the QEC codes targeting practically relevant errors in a hardware-efficient way. For example, we can develop various efficient bosonic QEC codes to correct excitation loss errors,[1–4] which have been experimentally demonstrated using superconducting circuits[5–9] and trapped ions.[10]

With energy gap protection or engineered dissipation, some bosonic codes can continuously suppress practically relevant errors (e.g., excitation loss) and also provide a highly biased noise channel. For example, two component cat qubits can be stabilized to the code space by either a driven Kerr Hamiltonian, which is termed Kerr cats,[11] or an engineered driven two-photon dissipation, which is termed dissipative cats.[12] The stabilized cats can exponentially suppress bit-flip errors, because of the large separation of coherent states in the phase space.[7,8,13] Such an encoding with highly biased noise channel can play a unique role in fault-tolerant architecture,[14,15] as the higher-level QEC codes can be tailored toward the biased noise to exhibit significantly improved error threshold and resource overhead. To get the maximum benefit from biased noise, it is essential for all gate operations to preserve the noise bias. Recently, a non-trivial set of bias-preserving (BP) gates have been discovered for stabilized cat qubits,[8,11,12,16] which opens up a new direction of fault-tolerant architectural design.[17–19]

However, both types of stabilized cat qubits have there own practical limitations. The dissipative cats, benefiting from the dissipative nature, can robustly suppress the minor errors and maintain large noise bias. However, while implementing the BP gates, the drives can stochastically produce major errors when combined with the white engineered dissipation. The above non-adiabatic effect, together with the relevantly weak engineered dissipation achievable by experiments, significantly limits the gate speed and leads to low gate fidelity. The Kerr cats, on the other hand, can support fast gates with high fidelity since the non-adiabatic effects are suppressed by the

Quantum Computing, Communication, and Simulation II, edited by Philip R. Hemmer, Alan L. Migdall, Proc. of SPIE Vol. 12015, 120150B · © 2022 SPIE
0277-786X · doi: 10.1117/12.2614832

large energy gap separating the ground states and the excited states. However, the Kerr cats, without careful control, could have lower noise bias due to leakage outside the code space. Intuitively, the Kerr Hamiltonian can be viewed as a double-well potential in phase space, with the cat states being the degenerate ground states. The minor errors are associated with the population transfer between two potential wells. The population transfer within the ground-state manifold is typically negligible since the ground states are well localized. However, the leakage to more delocalized excited states could lead to significantly increase bit-flip errors. The fast BP gates, without careful control, could coherently lead to such leakage. Furthermore, the interaction with the environment could also lead to accumulated leakage if no additional cooling is applied.

In this work, we summarize our results in Ref. citenumxu2021engineering, putterman2021colored, which introduce techniques to overcome the obstacles for Kerr-cat qubits and show that the fine-controlled Kerr cats can enjoy high noise bias and high-fidelity gates simultaneously. Specifically, in Sec. 2, we introduce the derivative-based controls for the BP gates that can coherently suppress the gate leakage. We show that the fine-controlled BP gates can have simultaneous high fidelity and high noise bias in the presence of excitation loss. Furthermore, We show how the fine-controlled BP gates on Kerr cats can significantly boost the logical code performance when the Kerr-cat qubits are concatenated with an outer QEC code. In Sec. 3, we introduce the colored (i.e., frequency-dependent) single-photon dissipation to suppress the environment-induced leakage of Kerr cats. We show that by adding frequency selective single photon loss we can continuously cool the Kerr cat to its ground state manifold without inducing errors on the logical information. Importantly, the colored dissipation is compatible with the aforementioned fast gate control due to the frequency separation between the narrow-band bath and the non-adiabatic drives.

2. FAST BIAS-PRESERVING GATES ON KERR-CAT QUBITS

2.1 Kerr/Dissipative cats and bias-preserving gates

In this section we briefly review the Kerr and dissipative cats and the set of BP gates proposed in earlier work. We discuss the properties and limitations of the existing BP gates, which motivates us to design better gate controls.

The cat qubit spanned by coherent states $|\alpha\rangle$ and $|-\alpha\rangle$ can be stabilized in a Kerr oscillator with parametric two-photon drive.[8,11,16,20] The Hamiltonian of such a Kerr parametric oscillator (KPO) in the frame rotating at the oscillator frequency is:

$$\hat{H}_{\mathrm{KPO}} = -K(\hat{a}^{2\dagger} - \alpha^2)(\hat{a}^2 - \alpha^2), \tag{1}$$

where K is the strength of Kerr nonlinearity. We may intuitively view the KPO system as a "double-well" potential with two extrema α and $-\alpha$ in phase space, as shown in Fig. 1(a). In addition to the degenerate ground states $|\pm\alpha\rangle$, $\hat{H}_{\mathrm{KPO}}$ supports nearly degenerate pairs of excited states with eigenenergies $\Delta_n \pm \delta_n/2$ for $n = 1, 2, \cdots$, where $\pm$ labels the photon-number parity and δ_n denotes the energy splitting between the n-th pair, which is exponentially suppressed by α^2 for $n < \alpha^2/4$.[16] denote the the subspace spanned by the n-th pair of (quasi-degenerate) excited states as the n-th excited subspace. The excitation gap $\Delta_1 \approx -4K|\alpha|^2$ * provides continuous protection of the encoded quantum information.

Alternatively, the cat qubit can also be stabilized by engineered two-photon dissipation and two-photon drive:[12,13,17]

$$\frac{d\rho}{dt} = \kappa_2 \mathcal{D}\left[\hat{a}^2 - \alpha^2\right]\rho, \tag{2}$$

where κ_2 is the two-photon dissipation rate and $\mathcal{D}[\hat{A}]\hat{\rho} = \hat{A}\hat{\rho}\hat{A}^\dagger - \frac{1}{2}\{\hat{A}^\dagger\hat{A}, \hat{\rho}\}$. We may intuitively understand the stabilization using a semi-classical flow diagram with two stable steady states $|\pm\alpha\rangle$ as illustrated in Fig. 1(b). For quantum evolution, the cat code space is stabilized as an attractive steady-state subspace protected by a dissipative gap.

By choosing the computational basis of the stabilized cat qubit as $|0\rangle_L \equiv \frac{|\psi_0^+\rangle + |\psi_0^-\rangle}{\sqrt{2}} \approx |\alpha\rangle, |1\rangle_L \equiv \frac{|\psi_0^+\rangle - |\psi_0^-\rangle}{\sqrt{2}} \approx |-\alpha\rangle$, the noise channel is strongly biased toward phase flip error $\hat{Z}$, with the noise bias $\eta \equiv P_z/P_x$ increasing

*Despite the energy gap $\Delta_1 < 0$ is negative in the rotating frame, the excitation energy $\omega_0 + \Delta_1 > 0$ is still positive in the lab frame, with oscillator frequency ω_0.

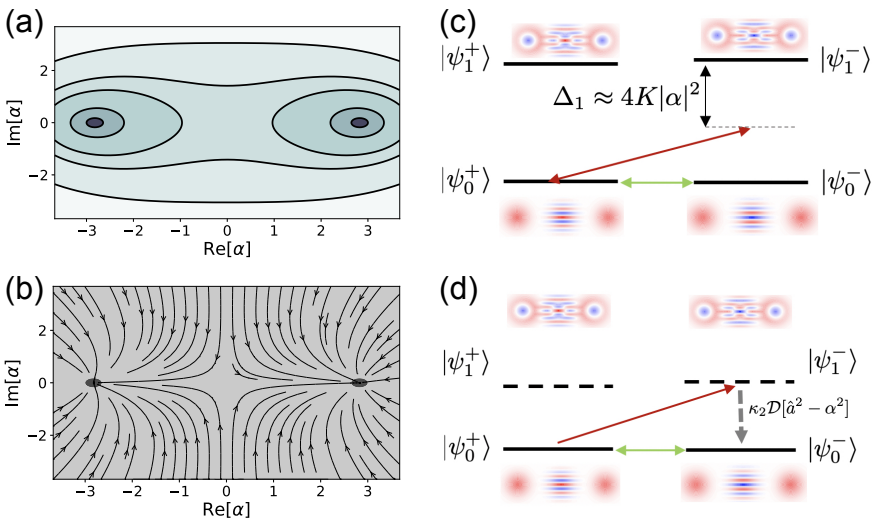

Figure 1. (a). The semi-classical potential $\langle \hat{H}_{\mathrm{KPO}} \rangle$ of a Kerr cat in phase space. (b). The semi-classical dynamics of a dissipative cat in phase space. (c)(d). Mechanism of the non-adiabatic errors during the Z-axis rotation on (c) Kerr cats and (d) dissipative cats. $|\psi_0^{\pm}\rangle, |\psi_1^{\pm}\rangle$ denote the first two pairs of eigenstates of $\hat{H}_{\mathrm{KPO}}$ with parity $\pm$ and the spacing between states in the vertical axis in (c) and (d) represents the energy gap and dissipative gap of the Kerr cat and the dissipative cat, respectively. For Kerr cats in (c), the non-adiabatic errors induced by the linear drive $(\Omega(t)\hat{a} + h.c.)$ manifest in the form of off-resonant leakage. While for dissipative cats in (d) with a dissipation gap, the linear drive induces decoherence within the cat state manifold when combined with the engineered two-photon dissipation.

exponentially with $|\alpha|^2$.[7,8,13] Here, and in the rest of the paper, we use P_x to denote the probability of all the non-dephasing type of errors for simplicity.

A set of bias-preserving gates have been proposed separately for Kerr cat[16] and dissipative cat,[12] which we refer to as Kerr gates and dissipative gates, respectively. Under excitation loss, the total Z and X error probabilities of the BP gates can be written as the following:[12,16,18]

$$\begin{aligned} P_z &= P_z^{\mathrm{NA}}(T) + \beta\kappa_1|\alpha|^2 T \\ P_x &= P_x^{\mathrm{NA}}(T) + \gamma\kappa_1|\alpha|^2 T, \end{aligned} \tag{3}$$

where κ_1 denotes the photon loss rate and β is a constant depending on the gate ($\beta = 1$ for Z rotation and $\beta = 2$ for ZZ rotation and CX gate). The first terms P_z^{NA} and P_x^{NA} are the non-adiabatic errors due to finite gate time and prefer slow gates, while the second terms are photon-loss-induced errors that increase with gate duration. The loss-induced bit flip is negligible since the induced bit-flip rate is suppressed by a factor $\gamma = \gamma[|\alpha|^2, \kappa_1/K(\kappa_2)] \ll 1$, which decreases exponentially for large $|\alpha|^2$,[7,12] and thereby P_x is dominantly given by P_x^{NA}. Here, we choose the size of the cat as $\alpha^2 = 8$, which is experimentally feasible[8] and also provides us sufficient noise bias.[16,18] Due to the large loss-induced phase flip rate, fast gates are desirable to obtain high gate fidelity. However, the exponential noise bias might break down in the fast-gate regime due to P_x^{NA}. Therefore, it is important to design fast BP gates with simultaneously suppressed P_z^{NA} and P_x^{NA}.

We would like to point out a fundamental difference in the non-adiabatic errors between Kerr gates and dissipative gates. For dissipative gates, the non-adiabatic errors are associated with accumulated dissipation with continuous information leakage into the environment, which is difficult to restore. For example, as shown in Fig. 1(d), the linear drive $\Omega(t)a + \Omega^*(t)a^\dagger$, which implements the Z rotation, can create leakage outside the cat subspace, which becomes continuous phase flips[18] when brought back by the engineered two-photon dissipation. In contrast, for Kerr gates shown in Fig. 1(c), the non-adiabatic errors are coherent off-resonant leakage errors to excited states, which might be reliably eliminated using additional leakage-suppression techniques. Hence, the Kerr gates can in principle benefit from quantum coherent controls, while the dissipative gates cannot.

As shown in Fig. 2, the Kerr gates with hard square pulses (blue curves, denoted as "Hard")[16] have smaller P_z^{NA} but larger P_x^{NA} than the corresponding dissipative gates (black dashed curves, denoted as "Dissipative").[12] The larger P_x^{NA} error is due to the large leakage induced by the hard pulse, which leads to coherent tunneling between two wells of the KPO through high excited levels. These numerical results manifest the importance for finer control on the Kerr gates to further suppress the leakage, which motivates our work. Although numerical quantum optimal control method[21] can be applied to optimizing the gates, analytical solutions that can produce smooth and robust pulses and avoid large-scale numerical optimizations for large cats are desirable. We use derivative-based transition suppression technique,[22] which is a variant of the derivative removal by adiabatic gate (DRAG) technique and closely related to the idea of shortcut to adiabaticity (STA),[22–26] to suppress the leakage of the BP Kerr gates so that they can have simultaneous high gate fidelity and noise bias in the presence of photon loss. The key idea behind this technique is to use quantum interference to suppress the occupation of the excited states by adding corrections to the original Hamiltonian according to the derivatives of the original driving pulse. The details of the derivative-based controls are presented in the next section.

2.2 Derivative-based control of BP gates on Kerr cats

To simultaneously suppress the non-adiabatic bit and phase flip errors of the BP Kerr gates, it is important to identify the associated excited subspace that dominantly contributes to each type of error, respectively. The phase flip errors come from parity flips and the occupation of any excited subspace with inconsistant parity compared to the ground subspace leads to phase flip errors. Therefore, if the drive invoking the diabatic transitions changes the parity, such as the linear drive that is commonly used by the gates that we consider, the dominant error space is the excited subspace with the largest occupation, which is typically the lowest-lying excited subspace with the smallest energy gap. The bit flip errors, however, come from the tunneling between the two potential wells of $\hat{H}_{\mathrm{KPO}}$ (see Fig. 1(a)). As a result, the excitation to higher excited subspaces in which the eigenstates are more delocalized brings more bit-flip errors. In fact, the excitation to the the characteristic level $n_c \sim \alpha^2/4$ typically leads to most of the bit-flip errors, since n_c is the lowest-lying level with well-delocalized states just above the potential barrier,[16] below which the states are well localized while above which the occupation is weaker. For $\alpha^2 = 8$ considered in this work, $n_c = 2$. With the above understanding of the error source, we should design the gate controls in the way that can greatly suppress the leakage to the dominant excited subspaces for both bit and phase flip errors. The tailored controls for each gate are summarized in Sec. 2.2.1. See 27 for more details.

2.2.1 Gate Hamiltonians

To suppress the diabatic transitions, We first replace the hard square pulses with a family of truncated Gaussian pulses because of their favorable frequency selectivity and smoothness:[22]

$$\Omega_{G,m}(t) = A_m \left\{ \exp\left[-\frac{(t-T/2)^2}{2\sigma^2} \right] - \exp\left[-\frac{(T/2)^2}{2\sigma^2} \right] \right\}^m \tag{4}$$

where m is chosen such that all of the first $m-1$ derivatives of $\Omega_{G,m}$ start and end at 0, A_m is a normalization constant and σ is chose to be equal to T in this work. Then, we introduce the systematically designed derivative-based correction (DBC) Hamiltonian, $\hat{H}_{\mathrm{DBC}}$, to further suppress the leakage for each gate. We summarize our design of corrections below.

The Hamiltonian for the Z rotation in Ref. 16 is implemented by applying a linear drive (with hard pulses) to the KPO:

$$\hat{H}_{\mathrm{Z}} = -K\left(\hat{a}^{2\dagger} - \alpha^2\right)\left(\hat{a}^2 - \alpha^2\right) + \Omega_0(t)\hat{a}^\dagger + \Omega_0^*(t)\hat{a}, \tag{5}$$

where $\Omega_0(t)$ is the hard pulse with amplitude determined by the desired rotation angle. Based on the discussion before, the non-adiabatic phase flip errors dominantly come from the first excited subspace with the gap energy Δ_1 while the non-adiabatic bit flip errors mainly come from the second excited subspace with the gap energy Δ_2. To suppress the first-order transitions at these two frequencies, we first replace the base driving pulse $\Omega_0(t)$ with the truncated Gaussian pulse with the second-order smoothness $\Omega_{G,2}(t)$ (See Eq. 4), and then apply the derivative-based correction, which reshapes the pulse of the linear drive by adding derivatives of the base pulse, $\hat{H}_{\mathrm{DBC}} = u(t)\hat{a}^\dagger + u^*(t)a$, where

$$u(t) = -i\dot{\Omega}_{G,2}\left(\frac{1}{\Delta_1} + \frac{1}{\Delta_2}\right) - \frac{\ddot{\Omega}_{G,2}}{\Delta_1\Delta_2} + 0.07\frac{\Omega_{G,2}^3(t)}{\Delta_1^2} \tag{6}$$

The ZZ rotation proposed in Ref.[16] is implemented by applying a beam-splitter interaction (with hard pulses) between the control mode (with subscript c) and the target mode (with subscript t):

$$\begin{gathered}\hat{H}_{\mathrm{ZZ}}(t)=\hat{H}_0+\hat{V}(t),\\ \hat{H}_0=-K(\hat{a}_c^{2\dagger}-\alpha^2)(\hat{a}_c^2-\alpha^2)-K(\hat{a}_t^{2\dagger}-\alpha^2)(\hat{a}_t^2-\alpha^2),\\ \hat{V}(t)=\Omega_0(t)\hat{a}_c\hat{a}_t^\dagger+h.c.\end{gathered}\tag{7}$$

We find that the two-mode squeezing, which can also generates the ZZ rotation and has the same order of nonlinearity as the beam-splitter coupling, invokes fewer diabatic transitions and is thereby easier to deal with. So we first replace the beam-splitter term in the Hamiltonian with a two-mode squeezing term, i.e. $\hat{V}(t)\rightarrow\Omega_0(t)\hat{a}_c^\dagger\hat{a}_t^\dagger+h.c.$. Then we identify the dominant excited subspaces for phase and bit flip errors. We use the notation (i,j) to label the subspace given by the tensor product between the i-th subspace for the control mode and the j-th subspace for the target mode. The excitation to the $(1,0)/(0,1)$ subspace dominantly leads to phase flips on the control/target mode; The excitation to the $(1,1)$ subspace dominantly leads to the correlated phase flips; The excitation to the $(2,0)/(0,2)$ subspace dominantly produces the bit flips on the control/target mode. Therefore, we aim to suppress three set of transitions with corresponding gap frequencies $\Delta_a\equiv\Delta_1,\Delta_b\equiv 2\Delta_1,\Delta_c\equiv\Delta_1+\Delta_2$ ($\Delta_2\approx 2\Delta_1$) in order to suppress the above mentioned bit and phase flip errors (and the tensor product between them). To do this, we first replace the base driving pulse $\Omega_0(t)$ with the truncated Gaussian pulse with the third-order smoothness $\Omega_{G,3}(t)$, and then apply the derivative-based correction, which further reshapes the driving pulse of the two-mode squeezing by adding derivatives of $\Omega_{G,3}$, $\hat{H}_{\mathrm{DBC}}=u(t)\hat{a}_c^\dagger\hat{a}_t^\dagger+h.c.$, where

$$u(t)=-i\dot{\Omega}_{G,3}(t)\left(\frac{1}{\Delta_a}+\frac{1}{\Delta_b}+\frac{1}{\Delta_c}\right)+i\frac{\dddot{\Omega}_{G,3}(t)}{\Delta_a\Delta_b\Delta_c}-\ddot{\Omega}_{G,3}(t)\left(\frac{1}{\Delta_a\Delta_b}+\frac{1}{\Delta_a\Delta_c}+\frac{1}{\Delta_b\Delta_c}\right)+0.13\frac{\Omega_{G,3}^3(t)}{\Delta_a^2}.\tag{8}$$

The original Hamiltonian in Ref.[16] for the CX gate between two modes reads:

$$\begin{gathered}\hat{H}_{\mathrm{CX}}(t)=\hat{H}_{\mathrm{KPO}}^{(c)}+\hat{H}_{\mathrm{KPO}}^{(t)}(t)+\hat{H}_{cp},\\ \hat{H}_{\mathrm{KPO}}^{(c)}=-K\left(\hat{a}_{\mathrm{c}}^{\dagger 2}-\alpha^2\right)\left(\hat{a}_{\mathrm{c}}^2-\alpha^2\right),\\ \hat{H}_{\mathrm{KPO}}^{(t)}(t)=-K\left[\hat{a}_{\mathrm{t}}^{\dagger 2}-\alpha^2e^{-2i\phi(t)}(\frac{\alpha-\hat{a}_{\mathrm{c}}^\dagger}{2\alpha})-\alpha^2(\frac{\alpha+\hat{a}_{\mathrm{c}}^\dagger}{2\alpha})\right]\times\left[\hat{a}_{\mathrm{t}}^2-\alpha^2e^{2i\phi(t)}(\frac{\alpha-\hat{a}_{\mathrm{c}}}{2\alpha})-\alpha^2(\frac{\alpha+\hat{a}_{\mathrm{c}}}{2\alpha})\right],\\ \hat{H}_{\mathrm{cp}}=-\tfrac{1}{2}\dot{\phi}\frac{\left(2\alpha-\hat{a}_{\mathrm{c}}^\dagger-\hat{a}_{\mathrm{c}}\right)}{2\alpha}\left(\hat{a}_{\mathrm{t}}^\dagger\hat{a}_{\mathrm{t}}-\alpha^2\right),\end{gathered}\tag{9}$$

where $\hat{H}_{\mathrm{KPO}}^{(t)}(t)$ stabilizes the phase of the target mode conditioned on the control mode and $\hat{H}_{cp}$ serves as a compensation Hamiltonian that partially compensates the non-adiabatic effects coming from the fast controlled phase rotation. The phase rotation is set to be linear, i.e. $\dot{\phi}(t)=\Omega_0(t)$ with $\Omega_0(t)$ being some hard pulse.

In the adiabatic frame (in which the cat states with time-dependent phase span the ground subspace) that block diagonalizes $\hat{H}_{\mathrm{KPO}}^{(c)}+\hat{H}_{\mathrm{KPO}}^{(t)}(t)$, the term $\hat{H}_{\mathrm{cp}}$ invokes diabatic-transitions that lead to leakage outside the cat-state manifold. In contrast to the Z and ZZ rotation, the correction to the CX gate is more complicated and requires adding more physical correction terms to $\hat{H}_{DBC}$, because of the the non-trivial dynamics in the excited subspaces. We design the corrections to suppress the leakage to the $(1,0),(0,1),(1,1)$ excited levels, which is the dominant process for non-adiabatic phase and bit flip errors (the complicated structure of $\hat{H}_{\mathrm{KPO}}^{(t)}$ leads to the fact that the leakage to the above mentioned subspaces also contributes greatly to the bit-flip errors). To realize this, we first replace the linear phase rotation with a more smooth rotation with a fist-order Gaussian derivative, i.e. $\dot{\phi}(t)\rightarrow\Omega_{G,1}(t)$, and then apply the following derivative-based correction $\hat{H}_{DBC}$:

$$\begin{gathered}\hat{H}_{DBC}=\hat{H}_{\mathrm{DBC},0}+\hat{H}_{\mathrm{DBC},1}+\hat{H}_{\mathrm{DBC},1}+\hat{H}_{\mathrm{DBC},3},\\ \hat{H}_{\mathrm{DBC},0}=i\tfrac{d}{dt}[\tfrac{\dot{\phi}}{\Delta_{11}(t)}]\tfrac{\hat{a}_c-\hat{a}_c^\dagger}{4\alpha}\times(\hat{a}_t^\dagger\hat{a}_t-\alpha^2),\\ \hat{H}_{\mathrm{DBC},1}=c_1\tfrac{\dot{\phi}(1-\cos 2\phi)}{\Delta_{11}(t)}(\hat{a}+\hat{a}^\dagger),\\ \hat{H}_{\mathrm{DBC},2}=ic_2\tfrac{\dot{\phi}\sin 2\phi}{\Delta_{11}(t)}\left(\hat{a}_c^2-\hat{a}_c^{2\dagger}\right),\\ \hat{H}_{\mathrm{DBC},3}=c_3\tfrac{\dot{\phi}(t)}{\Delta_{11}(t)}\left[\left(e^{2i\phi(t)}-1\right)\hat{a}_t^{2\dagger}+\left(e^{-2i\phi(t)}-1\right)\hat{a}_t^2\right],\end{gathered}\tag{10}$$

where $\Delta_{11}(t)$ is the time-dependent energy gap of the (1,1) subspace in the adiabatic frame that approximately diagonalizes $\hat{H}^{(t)}_{\mathrm{KPO}}(t)$, c_1, c_2, c_3 are constants depending on the representation of the $\hat{a}$ operator in the Kerr-cat eigenbasis. See 27 for detailed expressions for $\Delta_{11}(t), c_1, c_2$ and c_3. The correction terms $\hat{H}_{DBC,i}, i = 0, 1, 2, 3$ are designed to address different diabatic transitions accordingly. The maximum order of nonlinearity required to implement these corrections is the same as the original Hamiltonian Eq. 9. We note that due to the high complexity of the CX Hamiltonain, we only derive corrections to suppress the leakage to low-lying excited subspaces while in principle, similar to the Z and ZZ rotation, further corrections can be added to suppress the leakage to higher-lying subspaces, e.g. (0,2)/(2,0)/(1,2)/(2,1) subspaces, which may further suppress the non-adiabatic errors, especially the bit-flip errors.

2.2.2 Non-adiabatic gate errors

To illustrate the improvement from the DBC control, we numerically compare the non-adiabatic Z (P_Z^{NA}) and X (P_X^{NA}) errors among different BP control schemes for quantum operations of Z rotation, ZZ rotation and CX gate in Fig. 2. Both the non-adiabatic Z and X errors of the Kerr gates with DBC control are significantly reduced.

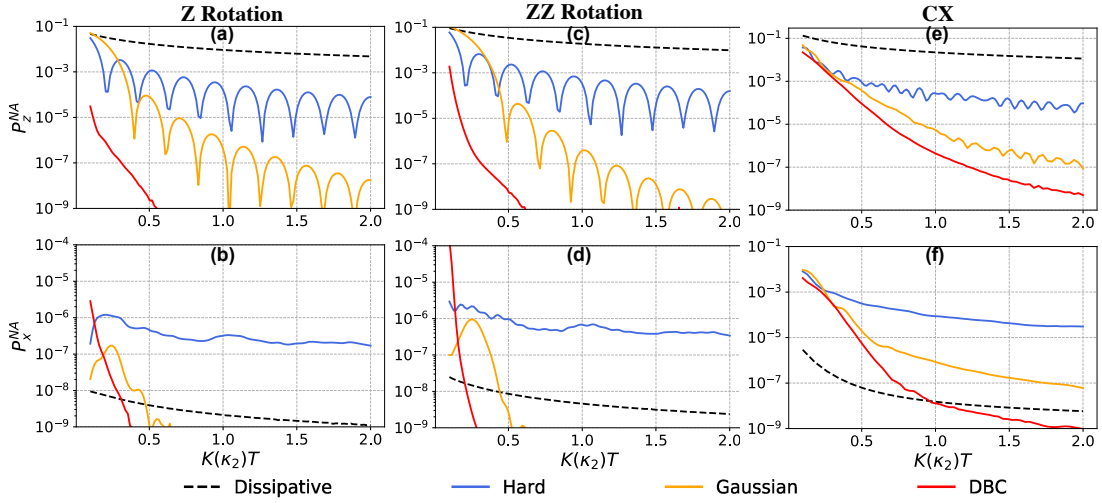

Figure 2. The non-adiabatic Z (P_Z^{NA}) and X (P_X^{NA}) errors of Z rotation (a)(b), ZZ rotation (c)(d) and CX gate (e)(f) for dissipative gates (black dashed curves), Kerr gates with hard square pulses (blue curves), truncated Gaussian pulses (orange curves), and DBC control (red curves). The gate time is in units of K (κ_2) for Kerr (dissipative) gates. The Kerr gates with DBC control can best suppress the non-adiabatic errors.

We explicitly provide the scaling of P_z^{NA} with the gate time below. For dissipative gates, $P_z^{\mathrm{NA}} \propto 1/\kappa_2 T$ is given by the integration the induced phase flip rate over gate time.[18] For Kerr gates with Hard/Gaussian control, $P_z^{\mathrm{NA}} \propto |\int_0^T \Omega_0(t) e^{-i\Delta t} dt|^2$ is dominated by the first-order diabatic excitation associated with an energy gap Δ, which is proportional to the Fourier component of the driving pulse at Δ (for the Z rotation $\Delta = \Delta_1$ while for the CX gate $\Delta = 2\Delta_1$). As such, $P_z^{\mathrm{NA}} \propto 1/(KT)^2$ for hard pulses, while for truncated Gaussian pulses P_z^{NA} first scales exponentially for small KT and then polynomially for large KT due to the sideband excitation.[22] And by adding derivative-based corrections to the bare Gaussian pulses we can dramatically suppress the excitation at Δ to the second order and maintain the exponentially error scaling in the regime of gate time of interest.

We note that since the bit flip errors mostly come from the non-adiabatic effects of the gates even in the presence of photon loss (which will be discussed in the next section), it is especially important to suppress the non-adiabatic bit flips so that the gates can be implemented fast while preserving high noise bias, which is the prominent feature that makes the biased-noise qubits stand out. For the Kerr CX gate, the hard pulses lead to significant non-adiabatic bit-flip errors due to the large excitation to high excited states, therefore almost destroying the noise bias (for fast gates). Using Gaussian pulses can noticeable reduce the non-adiabatic bit flips since high excitations are suppressed due to the limited bandwidth. By adding the derivative-based corrections

the excitations are further suppressed and as a result, the Kerr CX gate can have large noise bias (even larger than the dissipative gates) with fast implementation ($T \sim 1/K$). To achieve the same level of bit-flip error, the DBC control can be much faster than the Gaussian control, and consequently has lower loss-induced dephasing errors – which is crucial to reduce the resource overhead for concatenated QEC (see Sec. 2.3).

2.2.3 Gate performance in the presence of photon loss

In the presence of photon loss, the total Z error probability (Eq. 3) will have a significant new contribution ($\sim \kappa_1|\alpha|^2 T$), associated with the loss-induced parity change. In contrast, the total X error probability is still dominant by the non-adiabatic error P_x^{NA}. In Fig. 3, we numerically obtain Z and X error probability of CX gates at different gate time with $\kappa_1/K(\kappa_2) = 5 \times 10^{-5}$ and 5×10^{-4}.

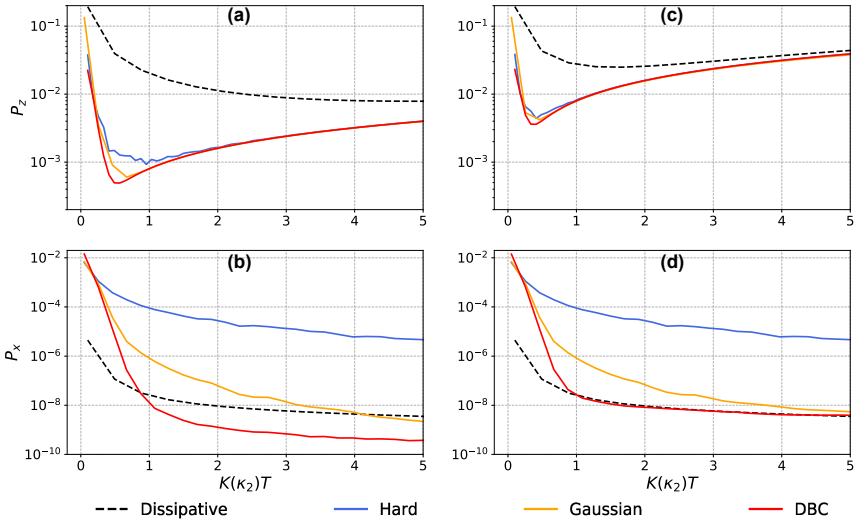

Figure 3. The total Z and X error probabilities for CX gate using different control schemes (same color scheme as Fig. 2) in the presence of photon loss. (a)(b): $\kappa_1/K(\kappa_2) = 5 \times 10^{-5}$. (c)(d): $\kappa_1/K(\kappa_2) = 5 \times 10^{-4}$. The gate time is in units of K (κ_2) for Kerr (dissipative) gates.

The total Z error probability P_z determines the gate fidelity. According to Eq. 3, the gate time can be optimized to minimize the total Z error probability. The Kerr gate can be implemented faster with higher gate fidelity than the dissipative gate and compared to using Hard/Gaussian control, using DBC control can further speed up the gate and improve the gate fidelity. Plugging in the scaling of P_z^{NA} with T we can obtain the scaling of the minimal Z error probability P_z^* with $\kappa_1/K(\kappa_2)$. For dissipative gates, $P^*_{z,\mathrm{Dissi}} \propto (\frac{\kappa_1}{\kappa_2})^{1/2}$. For Kerr gates with Hard control, $P^*_{z,\mathrm{Hard}} \propto (\frac{\kappa_1}{K})^{2/3}$. While for Kerr gates with Gaussian/DBC control, $P^*_{z,\mathrm{Gaussian}}/P^*_{z,\mathrm{DBC}}$ can approach the most favorable linear scaling, i.e. $P^*_{z,\mathrm{Gaussian}}/P^*_{z,\mathrm{DBC}} \propto \frac{\kappa_1}{K}$, with $P^*_{z,\mathrm{DBC}}$ being smaller. Given the same small parameter $\kappa_1/K(\kappa_2)$, our fine control scheme can provide a smaller Z error probability and thus a more favorable optimal gate fidelity.

The total X error probability P_x limits the noise bias of the gates. Compared to the dissipative gate, the P_x of the Kerr gate with Hard control is too high (at reasonable gate time). In contrast, the Kerr CX gate with Gaussian/DBC control can have P_x comparable to or even below that of the dissipative gate. In terms of gate time, the (counter-adiabatic) DBC control significantly out-perform the Gaussian control (limited by the adiabatic requirement). Hence, the DBC control can achieve faster gate with favorable noise bias.

2.3 Concatenated quantum error correction using repetition-Kerr-cat

We now compare the performance of different schemes of BP gates in terms of the logical gate failure rates in concatenated QEC. We consider the concatenation of the stabilized cats with a repetition code and simulate the logical gate failure rate using a circuit-level noise model, which includes state preparation errors, idling errors,

CX gate errors and measurement errors. The physical Z and X error rates of these operations are summarized in Tab. 1. The Z errors of the CX gate comprise of three parts: the Z error on the control mode which results from both non-adiabaticity and photon loss, the Z error on the target mode and correlated Z errors which are induced only by photon loss. $p_0 = \kappa_1|\alpha|^2 T_{\rm cx}$ is the characteristic photon-loss-induced Z error probability. For a distance-d repetition code we repeat the syndrome extraction d times followed by one round of perfect syndrome extraction (assuming no ancilla errors), decode the full error syndromes using a minimum weight perfect matching (MWPM) decoder for our noise-biased system and correct the errors by simply updating the Pauli frame.

Table 1. The physical error rates of different operations in our error model. $p_0 = \kappa_1|\alpha|^2 T_{\rm cx}$ is the characteristic Z error rate. The state preparation and measurement in the X basis do not produce bit flip errors and the bit flip error generated during the idling is negligible compared to that generated during the CX gate.

Operation	Idle	$\mathcal{P}_{\|+\rangle}$	$\mathcal{M}_X$	CX
P_z	p_0	p_0	p_0	$Z_c : p_z^{NA}(T_{\rm CX}) + p_0 \;\; Z_t : \frac{1}{2}p_0;\; Z_c Z_t : \frac{1}{2}p_0$
P_x	≈ 0	0	0	$p_x(\kappa_1, T_{\rm CX})$

We consider the total logical error rate of a transversal logical CX gate, which is a function of dimensionless parameters of the photon loss rate $\frac{\kappa_1}{K(\kappa_2)}$, the CX gate time $K(\kappa_2)T_{\rm CX}$, and the repetition code distance d. Given κ_1, we can obtain the minimum logical CX gate error rate achievable by the repetition-cat by optimizing $T_{\rm CX}$ and d (see 27 for details of the optimization):

$$P_L^{**}(\frac{\kappa_1}{K(\kappa_2)}) = \min_{T_{\rm CX},d} P_L(\frac{\kappa_1}{K(\kappa_2)}, K(\kappa_2)T_{\rm CX}, d). \tag{11}$$

In Fig. 4, we plot P_L^{**} and the corresponding optimal code distance d^{**} and gate time $T_{\rm CX}^{**}$ as a function of photon loss rate when different physical CX gates are used.

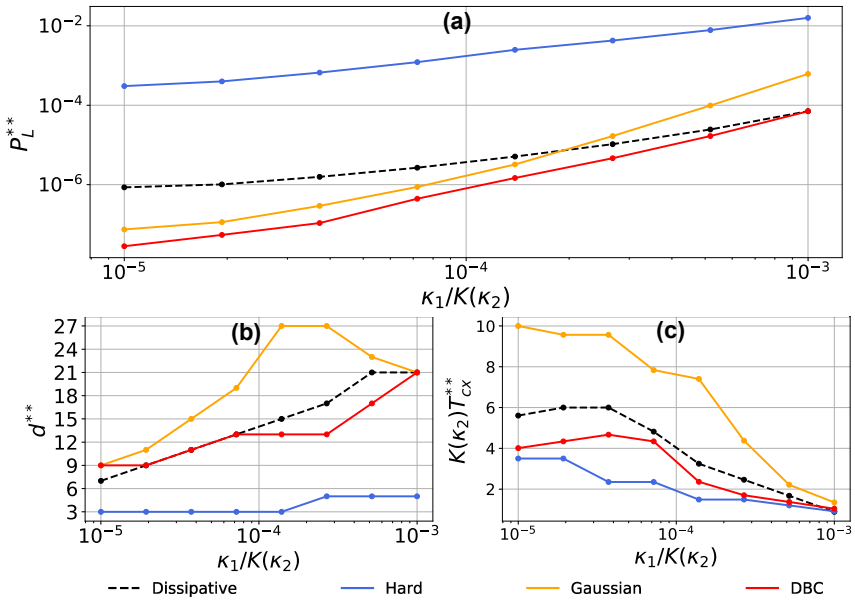

Figure 4. (a). The minimal gate error P_L^{**} of the logical CX gate using physical BP CX gates with different controls. (b)(c). The optimal choice of repetition-code distance (b) and the BP CX gate time (c) that minimizes the logical gate error.

Using the Kerr CX gates with DBC control can lead to the lowest logical gate error for $\kappa_1/K < 10^{-3}$, which outperforms all other schemes. The optimized P_L^{**} with dissipative gate is mostly limited by the large

P_z and the limited P_x in the low-loss regime (see Fig. 3a,c,b); the P_L^{**} based on Hard control is limited by the large non-adiabatic P_x error (see Fig. 3b,d); the P_L^{**} based on Gaussian control has to follow the adiabatic requirement with the longest gate time (see Fig. 4c), which leads to extra overhead in the size of repetition code d^{**} – especially for the practically relevant intermediate-loss regime ($\kappa_1/K \sim 10^{-4}$) in Fig. 4b. As expected, the Gaussian control should be comparable for the DBC control for extremely low loss regime ($\kappa_1/K \sim 10^{-5}$), which is compatible with slower adiabatic gates to maintain high gate performance.

Besides the logical error rates, we should also consider reduce the resource overhead required for reaching a target logical error rate when we consider other concatenation QEC schemes that can arbitrarily suppress logical errors, such as the surface-cat considered in Ref.[18,19] In this case, using the fast Kerr gates presented in this work can reduce the resource overhead towards fault tolerance since the dominant phase-flip errors are suppressed to be far below the threshold.

3. PROTECTING THE KERR CAT QUBITS FROM ENVIRONMENT-INDUCED LEAKAGE WITH COLORED DISSIPATION

In this section we introduce a new technique, called colored dissipation, to fight against the environment-induced leakage of the Kerr cat qubits. Unlike the non-adiabatic effects of the BP gates, the interaction with the environment inevitably introduces irreversible errors to the Kerr cats. Some errors, e.g. heating and dephasing, continuously lead to leakage of the Kerr cats. Such leakage, being incoherent and can not be suppressed by the energy gap, would accumulate and destroy the noise bias if no additional cooling was applied. We introduce the desired cooling effects by engineering colored dissipation. In particular, we show that by adding frequency selective single photon loss we can cool the Kerr cat to its ground state manifold without inducing errors on the logical information. In contrast to the two-photon dissipation protecting the dissipative cats that relies on nonlinear interactions, the colored dissipation can be readily implemented using passive and linear elements.

3.1 Shifted fock basis

In analyzing colored dissipation it is natural to think of a bosonic mode in terms of its subsystem decomposition. In such a decomposition we break the Hilbert space into two sectors. The first captures the logical information of the bosonic mode while the second "gauge" sector captures the degree to which the mode is excited above the ground state manifold. Here we briefly review the shifted-Fock basis[18] which naturally realizes such a decomposition for cat qubits. The shifted Fock basis consists of shifted Fock states $\hat{D}(\pm\alpha)|\hat{n} = n\rangle$ with $n \in \{0, 1, \cdots, d_{\max} - 1\}$, where $d_{\max}$ is the cutoff dimension. In the shifted Fock basis the annihilation operator is given by

$$\hat{a} = \hat{Z} \otimes (\hat{a}' + \alpha) + \mathcal{O}(e^{-2|\alpha|^2}). \tag{12}$$

Here, $\hat{Z}$ is a 2×2 Pauli Z operator acting on a qubit sector which describes the cat qubit logical information. $\hat{a}'$ is an annihilation operator acting on a gauge sector which captures how much the cat qubit is excited from the ground state manifold. The qubit sector of $\hat{a}$ is given by $\hat{Z}$ because in our basis convention, single-photon loss maps the complementary basis states $|\pm\rangle$ to $|\mp\rangle$ and hence causes a phase-flip (or Z) error on the logical information. In what follows, we assume that α is real. The Kerr-cat Hamiltonian in the shifted fock basis can be written as:

$$\begin{aligned}\hat{H}_{\mathrm{KC}} = &-4K\alpha^2\hat{I} \otimes \hat{a}'^{\dagger}\hat{a}' - K\hat{I} \otimes \hat{a}'^{\dagger 2}\hat{a}'^{2} \\ &- 2K\alpha\hat{I} \otimes (\hat{a}'^{\dagger 2}\hat{a}' + \hat{a}'^{\dagger}\hat{a}'^{2}) + \mathcal{O}(e^{-2\alpha^2}).\end{aligned} \tag{13}$$

In the limit of small excitations in the gauge sector (i.e., $\langle \hat{a}'^{\dagger}\hat{a}' \rangle \ll \alpha$), all but the first term in Eq. 13 can be neglected and the Kerr cat Hamiltonian is approximately reduced to that of a harmonic oscillator with an energy spacing $-4K\alpha^2$.

3.2 Environment-induced leakage and bit-flip errors for Kerr cats

Heating and dephasing are two dominant environment-induced errors that can cause leakage of the Kerr cats. Since dephasing and heating have similar effects, we only assume the existence of heating without loss of generality.[†] Heating of an oscillator can be modeled by the dissipator $\kappa_1 n_{\text{th}} \mathcal{D}[\hat{a}^\dagger]$. Since the creation operator $\hat{a}^\dagger$ is approximately given by $\hat{a}^\dagger \simeq \hat{Z} \otimes (\hat{a}'^\dagger + \alpha)$ in the shifted-Fock basis, heating induces phase flips and importantly leakage outside the code space due to the $\hat{a}'^\dagger$ term in the gauge sector (see Fig. 6 (a)).

In Fig. 6, we consider a set of experimentally relevant parameters: $K = 2\pi \times 10\text{MHz}$, $\kappa_1 = 2\pi \times 1\text{kHz}$ (corresponding to the lifetime of $1/\kappa_1 = 159\mu s$), and a thermal population $n_{\text{th}} = 0.1$ [‡]. As indicated by the blue line in Fi. 6 (b), the bit-flip error rate γ_X of a Kerr cat qubit stays constant throughout the range $3 \leq \alpha^2 \lesssim 9$, which are most experimentally relevant. This contrasts with expectations for exponential suppression of the bit-flip error rate γ_X with α^2 used throughout the literature for biased noise cat qubits.

To understand why the bit-flip error rate γ_X of a Kerr cat qubit does not improve as we increase α^2 up to 9, we need to consider the $\mathcal{O}(e^{-2\alpha^2})$ contributions in Eq. 13. In particular, we need to consider the terms in $\hat{H}_{\text{KC}}$ of the form $\chi_n \hat{X} \otimes |\hat{n}' = n\rangle\langle\hat{n}' = n|$. Here, χ_n can be understood as the tunneling rate between the states $|0\rangle \otimes |\hat{n}' = n\rangle$ and $|1\rangle \otimes |\hat{n}' = n\rangle$ (see the schematic Fig. 5). In Ref. 28 we show that the tunneling rate χ_1 in the first excited state manifold is perturbatively given by

$$\chi_1 \simeq 16 K \alpha^4 e^{-2\alpha^2}, \tag{14}$$

which agrees with the exact numerical results for all $\alpha^2 \geq 3$. Although χ_1 decreases exponentially in α^2, the large prefactor $16K\alpha^4$ can still make this χ_1 (induced by the Kerr cat Hamiltonian $\hat{H}_{\text{KC}}$) limiting in practice.

We now explain why the bit-flip error rate γ_X (blue line in Fig. 6 (b)) plateaus in the range $3 \leq \alpha^2 \lesssim 9$. Heating excites the system to the first excited state manifold. Here it persists for a time $\Delta t \sim 1/\kappa_1$ until it decays back to the cat state manifold. During this period, if $\chi_1 \gg \kappa_1$, rapid oscillations occur between the states $|0\rangle \otimes |\hat{n}' = 1\rangle$ and $|1\rangle \otimes |\hat{n}' = 1\rangle$. In this regime, a bit-flip error happens with 50% probability whenever heating creates an excitation. As a result, the bit-flip error rate is given by half the heating rate, i.e., $\gamma_X = \kappa_1 n_{\text{th}}/2$ in the regime of $\chi_1 \gg \kappa_1$. With our parameters (yielding $K/\kappa_1 = 10^4$), $\chi_1 = 16K\alpha^4 e^{-2\alpha^2}$ is at least 10 times larger than κ_1 for all $3 \leq \alpha^2 \leq 6.75$ and $\chi_1 = \kappa_1$ at $\alpha^2 = 8.08$. This explains why the bit-flip error rate γ_X is independent of α^2 and given by $\kappa_1 n_{\text{th}}/2$ in the range $3 \leq \alpha^2 \lesssim 9$. Above $\alpha^2 \sim 9$ heating to higher excited states becomes the important error mechanism because tunneling between the first excited states is sufficiently suppressed.

3.3 Colored Kerr-cat qubit

As shown by our numerical and analytical results, the heating-induced bit-flip errors can be even more detrimental than previously anticipated. Here, we propose to counteract the heating and leakage by adding frequency-selective (i.e., colored[29,30]) single-photon loss to Kerr cat qubits, hence making them *colored Kerr cat qubits*. Our scheme fundamentally differs from the previous proposals based on two-photon dissipation[8,19,31] as we only require single-photon loss. Intrinsic single-photon loss $\kappa_1 \mathcal{D}[\hat{a}]$ is harmful for cat qubits because the $+\alpha \hat{Z} \otimes \hat{I}$ term in the shifted-Fock basis representation of the annihilation operator $\hat{a} \simeq \hat{Z} \otimes (\hat{a}' + \alpha)$ causes phase-flip (or Z) errors in their ground state manifold.[11,13] The other term (i.e., $\hat{Z} \otimes \hat{a}'$) is useful for suppressing leakage as it brings the excited states back to the code space via $\hat{a}'$.

Our key idea is to engineer the frequency spectrum of the bath of the extrinsic single-photon loss such that we can take advantage of the beneficial decay term ($\hat{Z} \otimes \hat{a}'$) while filtering out the parasitic term ($+\alpha \hat{Z} \otimes \hat{I}$) from the single-photon loss $\hat{a}$. Since only the extrinsic single-photon loss is engineered with this technique, the intrinsic single-photon loss rate κ_1 should still be kept as small as possible.

[†]Dephasing $\kappa_\phi \mathcal{D}[\hat{a}^\dagger \hat{a}]$ can also lead to leakage but the energy gap suppresses $1/f$ noise. Furthermore dephasing and heating can be treated similarly so we focus on heating.[8]

[‡]The chosen values of K and n_{th} are close to those in Ref.[8] while the lifetime is 10x larger so it is in a known regime for fault tolerant quantum computation[19]

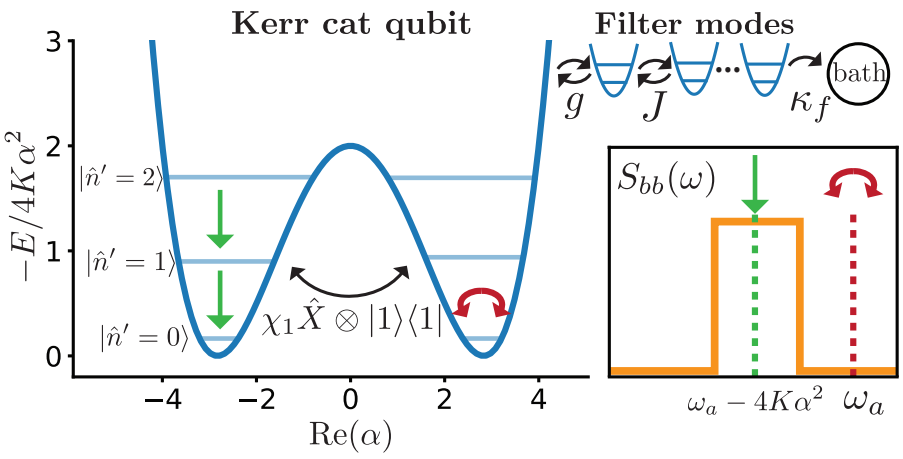

Figure 5. Schematic representation of a colored Kerr cat qubit, i.e., a Kerr cat qubit protected by frequency-selective (colored) single-photon loss. As shown in the inset, the harmonic filter modes are designed such that the colored single-photon loss realizes the desired cooling process (green arrow) while not inducing any additional phase-flip errors in the cat qubit manifold (red arrow). The black arrow in the schematic energy diagram represents the tunneling process between the first excited states, which is important for understanding the bit-flip rate of a Kerr cat qubit.

To demonstrate how our scheme works, we introduce a concrete setup where a Kerr cat qubit is coupled to an engineered bath through a set of harmonic filter modes with nearest-neighbor hopping, forming a colored Kerr cat qubit (see the schematic diagram in Fig. 5). Specifically, we consider the following Lindblad equation in the rotating frame of a Kerr cat qubit ($\hat{a}$ with frequency ω_a) and filter modes ($\hat{f}_1, ..., \hat{f}_M$ with frequency ω_f):

$$\begin{aligned}\frac{d\hat{\rho}(t)}{dt} &= -i[\hat{H},\hat{\rho}(t)] + \kappa_1(1+n_{\mathrm{th}})\hat{D}[\hat{a}]\hat{\rho}(t) \\ &\quad + \kappa_1 n_{\mathrm{th}}\hat{D}[\hat{a}^\dagger]\hat{\rho}(t) + \kappa_f\mathcal{D}[\hat{f}_M]\hat{\rho}(t),\end{aligned} \tag{15}$$

where the Hamiltonian $\hat{H}$ is given by

$$\hat{H} = \hat{H}_{\mathrm{KC}} + \Big[g\hat{a}\hat{f}_1^\dagger e^{i\Delta t} + J\sum_{j=1}^{M-1}\hat{f}_j\hat{f}_{j+1}^\dagger + \mathrm{h.c.}\Big]. \tag{16}$$

Here, $\Delta \equiv \omega_f - \omega_a$ is the detuning between the filter modes $\hat{f}_1, \cdots, \hat{f}_N$ and the mode $\hat{a}$ which hosts the Kerr cat qubit. Also, $\mathcal{D}[\hat{A}]\hat{\rho} \equiv \hat{A}\hat{\rho}\hat{A}^\dagger - \frac{1}{2}\{\hat{A}^\dagger\hat{A},\hat{\rho}\}$ is the Lindblad dissipator. Besides having the intrinsic loss and heating processes, the Kerr cat qubit can lose an excitation to the first filter mode at a rate g. Such an excitation is then transported to the last filter mode at a hopping rate J where it decays to a cold bath at a rate κ_f. It is important that this bath and the filter modes have a temperature much lower than the Kerr cat qubit so as to not induce additional heating (here $n_{\mathrm{th,filter}} = 0$). In particular, we choose $\kappa_f = 2J$ such that the filter modes act as an ideal band-pass filter (centered at the frequency ω_f and with a bandwidth $4J$) in the $N \to \infty$ limit.

Recall that in the shifted Fock basis, the Kerr cat Hamiltonian is approximately given by $\hat{H}_{\mathrm{KC}} \simeq -4K\alpha^2\hat{I}\otimes\hat{a}'^\dagger\hat{a}'$. Transforming to the shifted-Fock basis, and moving into the rotating frame of the $\hat{a}'$ mode the coupling term $g\hat{a}\hat{f}_1^\dagger e^{i\Delta t}$ becomes $g(\hat{Z}\otimes\hat{a}')\hat{f}_1^\dagger e^{i(\Delta+4K\alpha^2)t} + g\alpha(\hat{Z}\otimes\hat{I})\hat{f}_1^\dagger e^{i\Delta t}$. The first term realizes a desired cooling effect through $\hat{a}'$ whereas the second term causes undesired phase-flip (or Z) errors in the cat qubit manifold. By choosing $\Delta = -4K\alpha^2$ (or equivalently $\omega_f = \omega_a - 4K\alpha^2$), we can make the desired first term resonant while making the undesired second term off-resonant. Furthermore, by ensuring that the half bandwidth $\kappa_f = 2J$ is smaller than the detuning $|\Delta|$, we can place the undesired second term outside the filter passband and filter it out (see Fig. 5). In particular, through adiabatic elimination, the induced phase-flip error rate due to the second term is given by $(4g^2\alpha^2/\kappa_f)\times(J/\Delta)^{2M}$ in the $\Delta \gg J$ limit and hence decreases exponentially in the number

of the filter modes M. On the other hand, the resonant desired term realizes an engineered cooling process $\kappa_{1,\mathrm{eng}}\mathcal{D}[\hat{Z}\otimes\hat{a}']$ with an effective cooling rate $\kappa_{1,\mathrm{eng}}=4g^2/\kappa_f$.

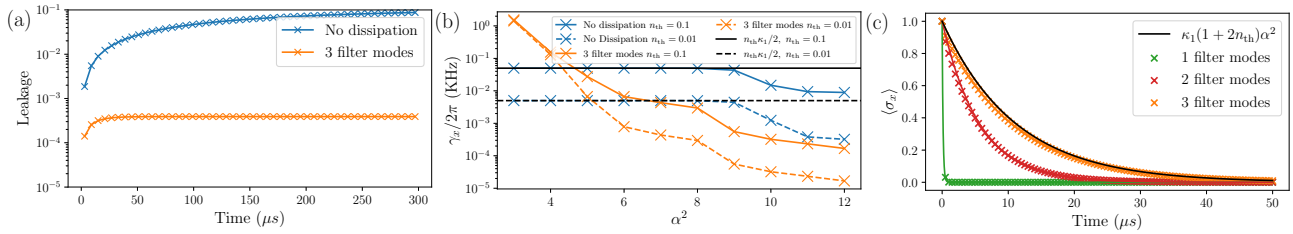

Figure 6. (a) Leakage accumulation over time in a Kerr cat qubit without any engineered dissipation (blue) and a colored Kerr cat qubit with three filter modes (orange) from the initial state $|\alpha\rangle$. (b) Bit-flip error rate of a Kerr cat qubit (blue) and a colored Kerr cat qubit with three filter modes (orange) as a function of the average photon number α^2 for $n_{\mathrm{th}}=0.1$ and 0.01. Black lines represent the analytical prediction $\gamma_X=\kappa_1 n_{\mathrm{th}}/2$ for the regime $\chi_1\gg\kappa_1+\kappa_{1,\mathrm{eng}}$. (c) Total phase-flip probability of a colored Kerr cat qubit with one (green), two (red), and three (orange) filter modes. In all three plots, we use the parameters $K=2\pi\times 10\mathrm{MHz}$ and $\kappa_1=2\pi\times 1\mathrm{kHz}$. In (a) and (c), we further assume $n_{\mathrm{th}}=0.1$ and $\alpha^2=6$.

In Fig. 6, we study the performance of a bare Kerr cat qubit and colored Kerr cat qubits with varying number of filter modes. In particular for colored Kerr cat qubits, we choose $\kappa_f=2J=\Delta/5$ and $g=\kappa_f/5$ to filter out the induced phase-flip errors and guarantee the validity of the adiabatic elimination, respectively. Also, we choose $\Delta=-3.6K\alpha^2$ (instead of $\Delta=-4K\alpha^2$) to more closely target the $0\leftrightarrow 1$ transition of the Kerr excited states. With these parameters, we get a large engineered cooling rate of $\kappa_{1,\mathrm{eng}}=2\pi\times 1.15\alpha^2\mathrm{MHz}$ (e.g., $\kappa_{1,\mathrm{eng}}=2\pi\times 6.9\mathrm{MHz}$ at $\alpha^2=6$). As indicated by the orange line in Fig. 6 (a), the leakage population of a Kerr cat qubit (of size $\alpha^2=6$) can be made orders of magnitude smaller by adding a frequency-selective single-photon loss with three filter modes. Additionally, the idling bit-flip error rate is reduced by at least an order of magnitude for all $\alpha^2\geq 6$ (see Fig. 6 (b)). This is because the large engineered cooling rate dramatically reduces the lifetime of excited states (especially the first excited states) so that the condition $\kappa_1+\kappa_{1,\mathrm{eng}}\gg\chi_1$ is satisfied at lower values of α^2.

In Fig. 6 (c) we show the total phase-flip probability as a function of time with 1, 2, and 3 filter modes and $\alpha^2=6$. With only one or two filter modes, the induced phase-flip rate is much larger than the intrinsic phase-flip rate of $\approx\kappa_1(1+2n_{\mathrm{th}})\alpha^2$ (green and red lines). With three filter modes, however, the induced phase-flip rate is negligible and the total phase-flip probability is close to the intrinsic rate (orange line). The observed phase-flip probabilities are consistent with our analytical prediction on the induced phase-flip rate $(4g^2\alpha^2/\kappa_f)\times(J/\Delta)^{2M}$ in the $\Delta\gg J$ limit. Hence, Fig. 6 (c) demonstrates that with a properly engineered single-photon loss spectrum we can benefit from the desired cooling effects without inducing additional phase-flip errors.

4. DISCUSSIONS

So far, the experimental Kerr parametric nonlinear oscillator can achieve $\kappa_1/K\approx 10^{-3}$ (with $\kappa_1/2\pi\approx 10$ KHz, $K/2\pi\approx 6.7$ MHz),[8] which is slightly more favorable than the engineered two-photon dissipation with $\kappa_1/\kappa_2\approx 10^{-2}$ (with $\kappa_1/2\pi\approx 1.7$ KHz, $\kappa_2/2\pi\approx 170$ KHz),[32] partly because Kerr nonlinearity is less complicated to implement than the two-photon dissipation. Note that the single photon loss rate is fairly high in all these experiments,[7,8,32] to be further reduced in future devices. We expect that $\kappa_1/K(\kappa_2)\leq 10^{-4}$ (e.g., $\kappa_1/2\pi\approx 1$ KHz, $K/2\pi\approx 10$ MHz) can be achieved,[16,18] which will enable us to achieve high fidelity logical gates in concatenated QEC. We note that the fine gate controls could potentially be also applied to other codes that require the implementation of bias-preserving gates, e.g. the pair-cat code.[33]

The idea of colored dissipation can in principle be made more general. Beyond the direct benefits to the Kerr cat qubit we may further generalize our technique to a broader class of energy-gap protected qubits whose computational basis states are given by near degenerate ground states of an energy gapped qubit, which is an interesting future direction to consider.

ACKNOWLEDGMENTS

We thank Aashish Clerk, Kyungjoo Noh, Shruti Puri, Harry Putterman and Hugo Ribeiro for helpful discussions. We also thank Christopher Chamberland for useful comments and suggestions on the concatenated quantum error correction. We thank Arne L. Grimsmo, Matthew H. Matheny, and Gil Refael for useful comments on the manuscript. The authors are also grateful for the support of the University of Chicago Research Computing Center for assistance with the numerical simulations carried out in this work. We acknowledge support from the ARO (W911NF-18-1-0020, W911NF-18-1-0212), ARO MURI (W911NF-16-1-0349), AFOSR MURI (FA9550-19-1-0399), NSF (EFMA-1640959, OMA-1936118, EEC-1941583), NTT Research, and the Packard Foundation (2013-39273).

REFERENCES

[1] Gottesman, D., Kitaev, A., and Preskill, J., "Encoding a qubit in an oscillator," *Physical Review A* **64**, 012310 (2001).

[2] Leghtas, Z., Kirchmair, G., Vlastakis, B., Schoelkopf, R., Devoret, M., and Mirrahimi, M., "Hardware-efficient autonomous quantum error correction," *Physical Review Letters* **111**, 120501 (2013).

[3] Michael, M. H., Silveri, M., Brierley, R. T., Albert, V. V., Salmilehto, J., Jiang, L., and Girvin, S. M., "New class of quantum error-correcting codes for a bosonic mode," *Physical Review X* **6**(3), 031006 (2016).

[4] Albert, V. V., Noh, K., Duivenvoorden, K., Young, D. J., Brierley, R. T., Reinhold, P., Vuillot, C., Li, L., Shen, C., Girvin, S. M., Terhal, B. M., and Jiang, L., "Performance and structure of single-mode bosonic codes," *Physical Review A* **97**(3), 032346 (2018).

[5] Ofek, N., Petrenko, A., Heeres, R., Reinhold, P., Leghtas, Z., Vlastakis, B., Liu, Y., Frunzio, L., Girvin, S. M., Jiang, L., Mirrahimi, M., Devoret, M. H., and Schoelkopf, R. J., "Extending the lifetime of a quantum bit with error correction in superconducting circuits," *Nature* **536**(7617), 441–445 (2016).

[6] Hu, L., Ma, Y., Cai, W., Mu, X., Xu, Y., Wang, W., Wu, Y., Wang, H., Song, Y. P., Zou, C. L., Girvin, S. M., Duan, L. M., and Sun, L., "Quantum error correction and universal gate set operation on a binomial bosonic logical qubit," *Nature Physics* **15**(5), 503–508 (2019).

[7] Lescanne, R., Villiers, M., Peronnin, T., Sarlette, A., Delbecq, M., Huard, B., Kontos, T., Mirrahimi, M., and Leghtas, Z., "Exponential suppression of bit-flips in a qubit encoded in an oscillator," *Nature Physics* **16**(5), 509–513 (2020).

[8] Grimm, A., Frattini, N. E., Puri, S., Mundhada, S. O., Touzard, S., Mirrahimi, M., Girvin, S. M., Shankar, S., and Devoret, M. H., "Stabilization and operation of a kerr-cat qubit," *Nature* **584**, 205–209 (Aug 2020).

[9] Campagne-Ibarcq, P., Eickbusch, A., Touzard, S., Zalys-Geller, E., Frattini, N. E., Sivak, V. V., Reinhold, P., Puri, S., Shankar, S., Schoelkopf, R. J., Frunzio, L., Mirrahimi, M., and Devoret, M. H., "Quantum error correction of a qubit encoded in grid states of an oscillator," *Nature* **584**(7821), 368–372 (2020).

[10] Flühmann, C., Nguyen, T. L., Marinelli, M., Negnevitsky, V., Mehta, K., and Home, J. P., "Encoding a qubit in a trapped-ion mechanical oscillator," *Nature* **566**(7745), 513–517 (2019).

[11] Puri, S., Boutin, S., and Blais, A., "Engineering the quantum states of light in a kerr-nonlinear resonator by two-photon driving," *npj Quantum Information* **3**(1), 1–7 (2017).

[12] Guillaud, J. and Mirrahimi, M., "Repetition cat qubits for fault-tolerant quantum computation," *Physical Review X* **9**, 041053 (Dec 2019).

[13] Mirrahimi, M., Leghtas, Z., Albert, V. V., Touzard, S., Schoelkopf, R., Jiang, L., and Devoret, M., "Dynamically protected cat-qubits: a new paradigm for universal quantum computation," *New Journal of Physics* **16**, 045014 (2014).

[14] Tuckett, D. K., Bartlett, S. D., and Flammia, S. T., "Ultrahigh error threshold for surface codes with biased noise," *Physical review letters* **120**(5), 050505 (2018).

[15] Bonilla-Ataides, J. P., Tuckett, D. K., Bartlett, S. D., Flammia, S. T., and Brown, B. J., "The xzzx surface code," *arXiv preprint arXiv:2009.07851* (2020).

[16] Puri, S., St-Jean, L., Gross, J. A., Grimm, A., Frattini, N. E., Iyer, P. S., Krishna, A., Touzard, S., Jiang, L., Blais, A., and et al., "Bias-preserving gates with stabilized cat qubits," *Science Advances* **6**, eaay5901 (Aug 2020).

[17] Guillaud, J. and Mirrahimi, M., "Error rates and resource overheads of repetition cat qubits," *arXiv:2009.10756 [quant-ph]* (Sep 2020). arXiv: 2009.10756.

[18] Chamberland, C., Noh, K., Arrangoiz-Arriola, P., Campbell, E. T., Hann, C. T., Iverson, J., Putterman, H., Bohdanowicz, T. C., Flammia, S. T., Keller, A., and et al., "Building a fault-tolerant quantum computer using concatenated cat codes," *arXiv:2012.04108 [quant-ph]* (Dec 2020). arXiv: 2012.04108.

[19] Darmawan, A. S., Brown, B. J., Grimsmo, A. L., Tuckett, D. K., and Puri, S., "Practical quantum error correction with the xzzx code and kerr-cat qubits," (2021).

[20] Goto, H., "Universal quantum computation with a nonlinear oscillator network," *Physical Review A* **93**(5), 050301 (2016).

[21] Pinch, E. R., [*Optimal control and the calculus of variations*], Oxford University Press (1995).

[22] Motzoi, F. and Wilhelm, F. K., "Improving frequency selection of driven pulses using derivative-based transition suppression," *Physical Review A* **88**, 062318 (Dec 2013).

[23] Guéry-Odelin, D., Ruschhaupt, A., Kiely, A., Torrontegui, E., Martínez-Garaot, S., and Muga, J., "Shortcuts to adiabaticity: Concepts, methods, and applications," *Reviews of Modern Physics* **91**, 045001 (Oct 2019).

[24] Theis, L. S., Motzoi, F., Machnes, S., and Wilhelm, F. K., "Counteracting systems of diabaticities using drag controls: The status after 10 years (a)," *EPL (Europhysics Letters)* **123**, 60001 (Oct 2018).

[25] Motzoi, F., Gambetta, J. M., Rebentrost, P., and Wilhelm, F. K., "Simple pulses for elimination of leakage in weakly nonlinear qubits," *Physical Review Letters* **103**, 110501 (Sep 2009).

[26] Ribeiro, H., Baksic, A., and Clerk, A. A., "Systematic magnus-based approach for suppressing leakage and nonadiabatic errors in quantum dynamics," *Physical Review X* **7**, 011021 (Feb 2017).

[27] Xu, Q., Iverson, J. K., Brandao, F. G., and Jiang, L., "Engineering fast bias-preserving gates on stabilized cat qubits," *arXiv preprint arXiv:2105.13908* (2021).

[28] Putterman, H., Iverson, J., Xu, Q., Jiang, L., Painter, O., Brandão, F. G., and Noh, K., "Colored kerr cat qubits," *arXiv preprint arXiv:2107.09198* (2021).

[29] Marquardt, F., Chen, J. P., Clerk, A. A., and Girvin, S. M., "Quantum theory of cavity-assisted sideband cooling of mechanical motion," *Phys. Rev. Lett.* **99**, 093902 (Aug 2007).

[30] Murch, K. W., Vool, U., Zhou, D., Weber, S. J., Girvin, S. M., and Siddiqi, I., "Cavity-assisted quantum bath engineering," *Phys. Rev. Lett.* **109**, 183602 (Oct 2012).

[31] Puri, S., Grimm, A., Campagne-Ibarcq, P., Eickbusch, A., Noh, K., Roberts, G., Jiang, L., Mirrahimi, M., Devoret, M. H., and Girvin, S. M., "Stabilized cat in a driven nonlinear cavity: A fault-tolerant error syndrome detector," *Phys. Rev. X* **9**, 041009 (Oct 2019).

[32] Touzard, S., Grimm, A., Leghtas, Z., Mundhada, S. Reinhold, P., Axline, C., Reagor, M., Chou, K., Blumoff, J., Sliwa, K. Shankar, S., Frunzio, L., Schoelkopf, R. Mirrahimi, M., and Devoret, M. "Coherent oscillations inside a quantum manifold stabilized by dissipation," *Physical Review X* **8**(2), 021005 (2018).

[33] Albert, V. V., Mundhada, S. O., Grimm, A., Touzard, S., Devoret, M. H., and Jiang, L., "Pair-cat codes: autonomous error-correction with low-order nonlinearity," *Quantum Science and Technology* **4**(3), 035007 (2019).